Thomson rings in a disk

M. Cerkaski,[1] R. G. Nazmitdinov,[2,3] and A. Puente[2]
[1]*Department of Theory of Structure of Matter, Institute of Nuclear Physics PAN, 31-342 Cracow, Poland*
[2]*Departament de Física, Universitat de les Illes Balears, E-07122 Palma de Mallorca, Spain*
[3]*Bogoliubov Laboratory of Theoretical Physics, Joint Institute for Nuclear Research, 141980 Dubna, Russia*
(Received 20 March 2014; published 23 March 2015)

We discuss the basic principles of self-organization of a finite number of charged particles interacting via the $1/r$ Coulomb potential in disk geometry. The analysis is based on the cyclic symmetry and periodicity of the Coulomb interaction between particles located on several rings. As a result, a system of equations is derived, which allows us readily to determine with high accuracy the equilibrium configurations of a few hundred charged particles. For $n \gtrsim 200$, we predict the formation of a hexagonal core and valence circular rings for the centered configurations.

DOI: 10.1103/PhysRevE.91.032312 PACS number(s): 64.75.Yz, 36.40.Wa, 02.20.Rt, 82.70.Dd

The distribution of charged particles on a two-dimensional curved surface, considered first by Thomson [1], has attracted continuous attention for a decade [2]. This problem provides useful insights into the physics of quantum dots and Bose-Einstein condensates [3], topological defects [4–6], and colloidal systems, where colloidal particles self-assemble at the interface of two distinct liquids such as particle-stabilized [7] or charged-stabilized emulsions [8,9].

Considering the electron distribution in a circular harmonic oscillator classically, Thomson found that interacting electrons are self-assembled in a family of rings (shells) with a specific number of electrons due to equilibrium conditions. Thirty years later, Wigner [10] predicted the formation of an electron lattice in an infinitely three-dimensional (3D) extended system at low density. These problems have common roots related to the dominance of the Coulomb interaction over the kinetic energy. Both models play a major role in our understanding of equilibrium configurations of interacting particles in the case of a soft confinement and in the absence of confinement. Evidently, however, they are different with respect to the role played by the number of particles, boundary conditions, and symmetry. For an infinitely large box, the discrete translation symmetry is responsible for the ordered structure in the Wigner crystal. In a circular trap, with a finite number of electrons, the cyclic symmetry gives rise to the formation of shells. For finite systems, the role of confinement and its underlying symmetries are crucial for the formation of equilibrium configurations [11].

Thanks to modern technology, many ideas and concepts developed early can be analyzed with high accuracy. Recent experimental studies of the additional electron energies of a small number of electrons in a trap over a liquid-helium film [12] confirm the results obtained by means of classical Monte Carlo calculations for the harmonic-oscillator trap [13–15]. The results demonstrate that n point charges located on a ring create equidistant nodes as predicted by Thomson [1]. There are hundreds of papers on the self-organization of charged particles in disk geometry (a hard confinement) in different fields of physics and chemistry (see, for example, [3,6]) where various simulation techniques are used. Although a similar pattern is obtained for a hard-wall potential for $n \leqslant 50$ (c.f., [16]), the distribution of particles is very different from the one found for the harmonic-oscillator confinement. Such a deviation, noticed already a few decades ago [17], is not understood yet. Indeed, the results of numerical simulations are rather formal because they are not based on any well-established model, while neither the Thomson nor the Wigner model mentioned above is relevant there. In contrast to the harmonic-oscillator case, a consistent analysis of the shell pattern obtained by simulation techniques in disk geometry has been lacking up to now (for a review, see [18]). Among the latest developments, we could mention the approach based on a continuum limit [4,5]. Although this approach describes a general trend of the density distribution in the framework of elasticity theory, it is unable to provide a detailed description of the shell structure for a finite number of particles.

In this paper, we present a model that enables one to describe with high accuracy the ground-state configuration of charged particles in a disk as a function of particle number. Although we consider the classical system at zero temperature, our approach could shed light on the nature of self-organization of colloidal particles in organic solvents, charged nanoparticles absorbed at oil-water interfaces, and electrons trapped on the surface of liquid helium. To address the problem, we consider particles (electrons) confined in a planar disk and interacting via the Coulomb interaction. To check the validity of our theoretical approach, we also perform molecular-dynamics (MD) calculations similar to the one discussed in [18] and compare our predictions with the MD results for $n \leqslant 400$ particles.

The MD results indicate that for $n \leqslant 11$, the equilibrium configuration is defined by all particles equally distributed on the circle with radius R. In this case, the minimal energy of the system is

$$E_n(R) = \frac{\alpha}{2R}\sum_{i=1}^{n-1}\sum_{j=i+1}^{n}\frac{1}{\sin\frac{\pi}{n}(|i-j|)} = \frac{\alpha n S_n}{4R}, \quad (1)$$

$$S_n = \sum_{k=1}^{n-1}\frac{1}{\sin\frac{\pi}{n}k}. \quad (2)$$

Here, $\alpha = e^2/4\pi\varepsilon_0\varepsilon_r$. Below, for the sake of discussion, we use $\alpha = 1$, unless stated otherwise. We recall that with the harmonic-oscillator confinement, already for $n = 6$ one obtains one particle at the center $(5 + 1)$ [1,13–15].

Let us suppose that the system is stable with n particles located at the circle boundary. If we add a particle, then either (i) it is placed at the boundary with a total energy E_{n+1}, or (ii) due to circular symmetry it is located at the center, interacting with the external n charges, and the total energy is $E_n(R) + n/R$. The critical number of charged particles for this transition is defined by the condition $[E_n(R) + n/R] - E_{n+1}(R) \leqslant 0$, which yields the following equation:

$$(n+1)S_{n+1} \geqslant nS_n + 4n. \tag{3}$$

The resolution of this equation provides the critical number $n = 11$. In other words, 11 charged particles lie on the circle boundary, while for 12 charged particles there are 11 charged particles at the boundary and one is located at the center.

For $n \geqslant 12$, the MD calculations show the formation of several internal rings. In particular, for $n \leqslant 29$ the number of electrons grows in two rings until two complete shells (23 + 6) are formed. Evidently, the interaction between electrons from different rings should be included now. To obtain further insight into the formation of the equilibrium configuration, we consider the Coulomb interaction between two rings with radiuses r_1, r_2, and n and m electrons, respectively, uniformly distributed on each ring. Thus, we have

$$E_{nm}(r_1,r_2,\psi) = \sum_{i=1}^{n}\sum_{j=1}^{m} \epsilon\left(r_1,r_2,\psi_{ij}^{nm} + \psi\right), \tag{4}$$

$$\epsilon(r_1,r_2,\theta) = \left(r_1^2 + {r_2}^2 - 2\,r_1\,r_2\,\cos\theta\right)^{-1/2}, \tag{5}$$

where $\psi_{ij}^{nm} = 2\pi(i/n - j/m)$ and ψ is the relative angular offset between the two rings.

It can be shown that the set of $n \times m$ angles ψ_{ij}^{nm} is equivalent, in the interval $[0,2\pi]$, to the G-fold set $\{\psi_k = 2\pi/L \times k, k = 1,\ldots,L\}$. Here $L \equiv \mathrm{LCM}(n,m)$ and $G \equiv \mathrm{GCD}(n,m) = n \times m/L$ are the least common multiple and greatest common divisor of the numbers (n,m), respectively. As a result, Eq. (4) transforms to

$$E_{nm}(r_1,r_2,\psi) = G\sum_{k=1}^{L}\epsilon(r_1,r_2,\psi_k + \psi), \tag{6}$$

which can be applied to any 2π periodic function $\epsilon(r_1,r_2,\theta)$. In turn, this result shows that these kinds of functions are invariant under angle transformations corresponding to the cyclic group of L elements, implying a $\Delta_{nm} = 2\pi/L$ periodicity

$$E_{nm}(r_1,r_2,\psi + \Delta_{nm}) = E_{nm}(r_1,r_2,\psi). \tag{7}$$

This is a key result of our approach, which allows us to simplify drastically the problem of equilibrium configurations and underlines the importance of cyclic symmetry.

By virtue of the fact that the ring-ring interaction is an even periodic function in the angle ψ, it can be presented by means of a Fourier series of cosines,

$$E_{nm}(r_1,r_2,\psi) = \langle E_{nm}\rangle + \sum_{\ell=1}^{\infty} C_{\ell nm}(r_1,r_2)\cos(\ell L\psi). \tag{8}$$

The average value is obtained by integrating in ψ, and using Eq. (6) we have

$$\begin{aligned}\langle E_{nm}\rangle &= \frac{1}{2\pi}\int_0^{2\pi} d\psi\; E_{nm}(r_1,r_2,\psi)\\ &= \frac{G}{2\pi}\sum_{k=1}^{L}\int_0^{2\pi} d\psi\;\epsilon(r_1,r_2,\psi_k + \psi).\end{aligned} \tag{9}$$

All terms in the sum Eq. (9) give the same contribution, and we obtain in terms of the complete elliptic integral of the first kind [19]

$$\langle E_{nm}\rangle = \frac{2nm}{\pi r_>(1+t)}K[4t/(1+t)^2] = 2nm\frac{K(t^2)}{\pi r_>}. \tag{10}$$

Here, we introduced the following notations: $r_> = \max(r_1,r_2)$, $r_< = \min(r_1,r_2)$, $t = r_</r_>$, and we used the symmetry property $K[4t/(1+t)^2] = (1+t)\,K(t^2)$. It is noteworthy that the average value $\langle E_{nm}\rangle$ is exactly the interaction energy between homogeneously distributed n and m charges over the first and second rings, respectively.

In a similar way, the Fourier coefficients are given by

$$\begin{aligned}C_{\ell nm}(r_1,r_2) &= \frac{1}{\pi}\int_0^{2\pi} d\psi\;\cos(\ell L\psi)E_{nm}(r_1,r_2,\psi)\\ &= \frac{nm}{\pi}\int_0^{2\pi} d\psi\;\frac{\cos(\ell L\psi)}{\left[r_1^2 + r_2^2 - 2r_1r_2\cos\psi\right]^{1/2}}.\end{aligned} \tag{11}$$

By means of series expansion, it can be shown that

$$C_{\ell nm}(t) \approx \frac{nm}{r_>}d_{\ell L}t^{\ell L} + O(t^{\ell L+2}), \tag{12}$$

where $d_M = 2(2M-1)!!/(M!\,2^M)$ is a slowly decreasing coefficient. Evidently, at large L the contribution brought about by the fluctuations related to the ψ variable in the series (8) is very small, even for the first harmonic $\ell = 1$. For illustration, we consider the fluctuating part of the ring-ring energy,

$$\Delta E_{nm}(R,r) = \langle E_{nm}\rangle - E_{nm}(R,r,\psi = \pi/L) \tag{13}$$

for $m = 6$ in the internal ring with a radius r, and we vary the electron number $20 \leqslant n \leqslant 25$ in the external ring with a radius R.

From the numerical analysis (see Fig. 1) it follows that

$$\Delta E_{nm}(R,r) \sim c_L\,(r/R)^L, \tag{14}$$

which is fully consistent with the estimation (12). It is evident that fluctuations hardly play a role in the ring-ring interaction at large L, for instance when $n = 23$ ($L = 138$) or $n = 25$ ($L = 150$). Even for the worst case $n = 24$ ($L = 24$), it amounts to a small fraction of $\langle E_{nm}\rangle$ for ratios $r/R < 0.8$.

The results for two interacting rings guide us to tackle the issue of the total energy. The total energy of n charged particles in a disk of radius R is

$$\mathscr{E}_{\mathrm{tot}}(\mathsf{n},\mathsf{r},\boldsymbol{\varphi}) = \sum_{i=1}^{p}E_{n_i}(r_i) + \sum_{i<j}^{p}E_{n_in_j}(r_i,r_j,\varphi_i - \varphi_j). \tag{15}$$

Here, $\mathsf{n} = (n_1,\ldots,n_p)$ is a partition of the total number n on p rings with radiuses $\mathsf{r} = (r_1,\ldots,r_p)$ and offset angles

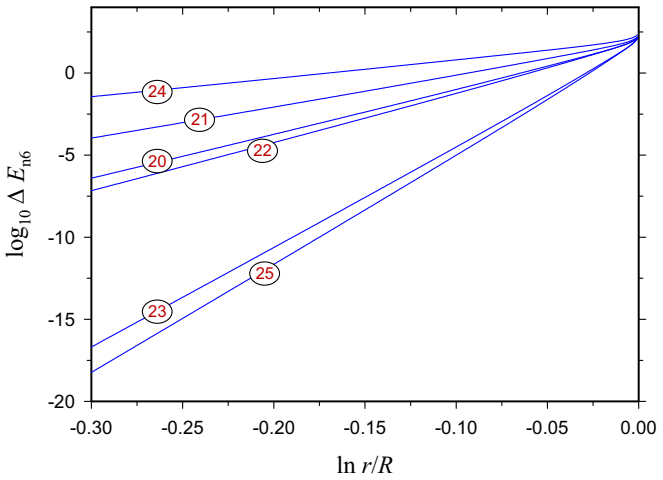

FIG. 1. (Color online) The fluctuation of ring-ring energy, Eq. (13), as a function of the ratio $x = r/R$ for $m = 6$ in the internal ring and $20 \leqslant n \leqslant 25$ in the external ring.

$\boldsymbol{\varphi} = (\varphi_1 = 0, \ldots, \varphi_p)$. We assume $R = r_1 = 1 > r_2 > \cdots > r_p$. The results for two rings suggest defining the total energy as $\mathscr{E}_{\rm tot}(\mathsf{n},\mathsf{r},\boldsymbol{\varphi}) = \mathscr{E}_{\rm avg}(\mathsf{n},\mathsf{r}) + \delta E(\mathsf{n},\mathsf{r},\boldsymbol{\varphi})$ with

$$\mathscr{E}_{\rm avg}(\mathsf{n},\mathsf{r}) = \sum_{i=1}^{p} n_i \frac{S_{n_i}}{4r_i} + \frac{2}{\pi}\sum_{i<j}^{p} n_i\, n_j\, \frac{K[(r_j/r_i)^2]}{r_i}, \qquad (16)$$

and neglecting the dependence on the relative angles $\psi = \varphi_i - \varphi_j$, i.e., the term $\delta E(\mathsf{n},\mathsf{r},\boldsymbol{\varphi})$.

The equilibrium configuration of particles can be obtained by minimizing the energy [see Eq. (16)] with respect to $(p,\mathsf{n},\mathsf{r})$, i.e., finding the partition corresponding to the lowest total energy. For a given partition, the set of equations $r_i\,\partial\mathscr{E}_{\rm avg}(\mathsf{n},\mathsf{r})/\partial r_i = 0$ that determines the optimal radiuses $(r_i, i = 2, \ldots, p)$ is

$$r_i^2 \sum_{j=i+1}^{p} \frac{n_j\, E[(r_j/r_i)^2]}{{r_j}^2 - r_i^2} + r_i \sum_{j=1}^{i-1} n_j \left(\frac{r_j\, E[(r_i/r_j)^2]}{r_j^2 - r_i^2} - \frac{K[(r_i/r_j)^2]}{r_j} \right) = \frac{\pi}{8} S_{n_i}. \qquad (17)$$

Here, E is the complete elliptic integral of the second kind. Thus, instead of searching for the optimal arrangement of n particles by means of simulation techniques, one must seek the partition n that provides the lowest value of $\mathscr{E}_{\rm avg}$ by solving a system of a few $(p-1)$ equations.

Numerical analysis of the system (16) and (17) shows that, once one electron appears at the center, it gives rise to a new internal ring (shell) that is progressively filling with electrons. The list of lowest-energy configurations with filled shells reads $n/\mathscr{E}_{\rm avg}\{\mathsf{n}\}$: 11/48.5757{11}; 29/444.548{23,6}; 55/1792.01{37,13,5}; 90/5115.56{53,20,12,5}; 135/11995.4{70,29,19,12,5}. The largest number of electrons lies on the circle boundary and decreases with sequential access to inner shells 2,3, ... The numerical solution of the system (16) and (17) provides a remarkable agreement with the MD calculations for equilibrium configurations up to $n = 105$, excluding a few cases (see Table I). Our MD results agree with those of Ref. [18] up to $n = 160$ particles, while we obtain lower energies for $n = 400,500,1000$ and also systematically better values for $n > 52$ than those implied in Fig. 8 of Ref. [5].

TABLE I. Values for the only seven cases in which optimal configurations, obtained with the aid of Eq. (17), disagree with the MD results. The MD results can be found also in [18].

n	$\mathscr{E}_{\rm avg}(n)$	δ	Configuration
38	805.021	−0.101404	$(28,9,1)_2^3$
61	2237.25	−0.056784	$(39,14,7,1)_3^1$
76	3575.38	−0.176466	$(46,17,10,3)_3^1$
79	3881.59	−0.164677	$(48,17,10,4)_4^2$
88	4878.17	−0.109206	$(51,20,12,5)_3^1$
90	5115.56	−0.155515	$(53,20,12,5)_1^5$
97	5991.62	−0.148982	$(55,21,13,7,1)_4^2$

The difference $\delta = E_{\rm MD} - \mathscr{E}_{\rm avg}$ provides the error of our approximation. The rings are counted starting from the external one, which is the first ring. The notation $(28,9,1)_2^3$ means that we have to add one particle in the third ring and remove one particle from the second ring in order to obtain the MD result. Although the total energy errors are very small, the assumptions of our model fail to predict the correct configurations for the shown total n. The reason for this is twofold. First, as discussed above, the fluctuating part [see Eqs. (8) and (11)] diminishes when L is large, while at small L its contribution may affect the prediction of the optimal configuration. Second, some MD configurations slightly break circular symmetry, which is not considered in the present approach. Nevertheless, we stress that in practical cases considered so far for $n \leqslant 400$, the solution of our equations (16) and (17) reduces the CPU time by a considerable factor (about 10^3 for $n \approx 400$) in comparison with the MD calculations. Moreover, with the aid of this solution as a guide for the initial MD particle positions, one reduces drastically the scanning effort to find the exact ground-state configurations. We recall that systematic studies of equilibrium configurations in a disk geometry with Monte Carlo simulation techniques and MD calculations have been done up to $n \leqslant 50$ [16] and $n \leqslant 160$ [18], respectively.

Starting from $n = 106$, the predictions based on the energy $\mathscr{E}_{\rm avg}$ and MD results demonstrate a systematic $\Delta n \approx |2|$ disagreement in the partition of charged particles between available rings. In particular, the particle number, which corresponds to the opening of a new shell (starting from one particle in the center), can be calculated exactly up to $n = 90$ with the aid of the formula $n = (2p+1)(2p+2)$ (see also [20]). It gives $n = 132$ at $p = 5$, while the MD results provide the opening of the sixth shell at $n = 134$. Our calculations predict this opening at $n = 136$. Nevertheless, by means of this formula one obtains an estimation of the shell number p associated with a given particle number $n > 90$: $p \simeq \sqrt{n}/2$.

The increase in the particle number gives rise to the onset of a centered hexagonal lattice (CHL) at the core of the disk (see also the discussion in [5,16,18]). In fact, for equilibrium configurations close to the one that opens a new shell, we find

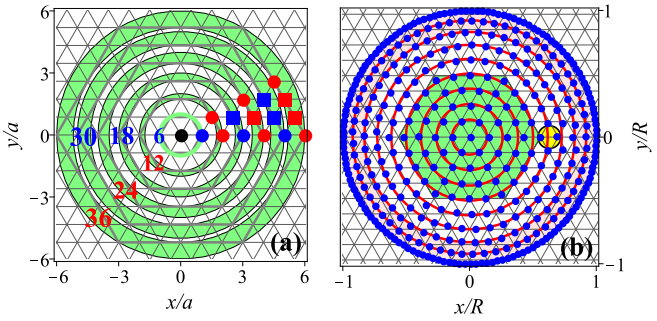

FIG. 2. (Color online) (a) Structure of internal (*core*) rings corresponding to the CHL. Each shell (green) contains a family of circles with radii R_{kl} and particle numbers $n_{\rm ring} = 6p$ (see the text). Solid dots and squares correspond to lattice sites with 6- and 12-fold multiplicity, respectively. (b) Comparison of the numerical solution of Eq. (17) (rings) with the MD results (dots) for $n = 395$ particles. The *core* (green) region with {**1**,**6**,**12**,**18**,**24**} particles exhibits a hexagonal pattern. The five external *valence* shells contain 147,65,50,40,32 particles with an almost perfect circular structure for the three outer rings (pink). There is a small mismatch, involving two particles at the intermediate region, displayed within the small (yellow) circle.

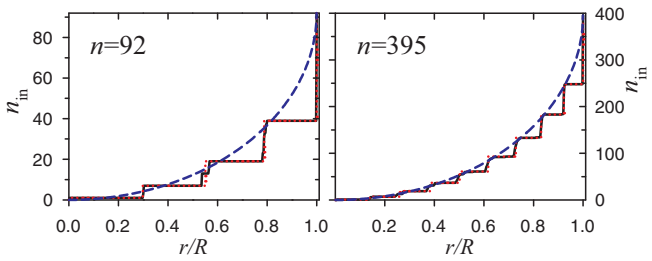

FIG. 3. (Color online) Number of charged particles within a disk of radius r. The results of MD, our model, and a continuum model [5] are shown, respectively, by a solid (black), dotted (red), and dashed (blue) line for $n = 92$ and 395 charges.

an increasing sequence of rings, starting from the center, with $n_k = 6k$ particles matching the regular hexagonal pattern. This is clearly seen in the results for $n = 92$ {**1**,**6**,**12**,20,53}, $n = 136$ {**1**,**6**,**12**,19,28,70}, $n = 187$ {**1**,**6**,**12**,**18**,26,37,87}, ..., $n = 395$ {**1**,**6**,**12**,**18**,**24**,32,40,50,65,147}. It is worth mentioning that the relative error in $\mathscr{E}_{\rm avg} = 110\,667.6$ for $n = 395$ with respect to the MD result (=110 665.1) is only 2×10^{-3}%. For even bigger systems, we find the formation of just seven full shells, $n = 1976${**1**, ..., **42**, ...}, before the symmetry of the circular confining geometry takes over.

This fact can be understood by considering the arrangement of the CHL points, $\vec{x}_{k,\ell} = k\vec{a}_1 + \ell\vec{a}_2$, given by integers k,ℓ and the two primitive Bravais lattice vectors $\vec{a}_1 = a(1,0)$ and $\vec{a}_2 = a(1/2,\sqrt{3}/2)$, where a is the lattice constant. The $n_p = 6p$ sites in the pth shell are organized in different circular rings with radii $R_{k\ell} = a\sqrt{k^2 + \ell^2 + k\ell}$, where $p = k + \ell$ and $0 \leqslant \ell \leqslant k$, containing either 6 (if $\ell = 0,k$) or 12 (otherwise) particles [see Fig. 2(a)]. Up to $p = 7$, all these radii are well ordered within and between successive shells, and the model we presented groups them in a single circular shell $n_{\rm ring} = 6p$. Beyond the seventh shell, however, rings start to overlap (e.g., $R_{7,0} > R_{4,4}$), ultimately distorting this sequence as they depart from the center.

A comparison of the predictions of our model with the MD results for $n = 395$ particles is shown in Fig. 2(b). The discrete equilibrium positions at the core of the structure are nicely located over a hexagonal lattice that gets progressively distorted as one moves toward the boundary, where particles are arranged in almost perfect circular shells. As discussed above, we consider the interaction of homogeneously distributed charges on several rings, neglecting the angular displacement between them. This zero-order approximation hides the mechanisms of topological defects [see Fig. 2(b), small (yellow) circle] discussed, for example, by Mughal and Moore [5] by means of a continuum model. This model neglects, however, finite-size fluctuations and is only appropriate for very large systems. In contrast, our model is able to reproduce the shell pattern obtained with MD calculations for any finite n remarkably well [see Table I and Figs. 2(b) and 3]. It is interesting to note that the number of charges in the outer shell (ring) fitted to our model data ($n \leqslant 400$) is well reproduced by the formula $n_{\rm out} = 2.795n^{2/3} - 3.184$ and confirms the power-law scaling obtained also in Refs. [5,18]. Similar scalings can also be found for subsequent shells as well as for the smooth part of the total energy. However, these fits should be taken cautiously, since the coefficients depend strongly on the fitting range and the quality of the data, which are assumed to correspond to the lowest-energy configuration. Further refinement of our method brought about by including the angular dependence and understanding of phenomenological coefficients requires a dedicated study and is a subject of a forthcoming paper.

Increasing the particle number at fixed R, one reaches the situation in which quantum corrections due to electron zero-point fluctuations, $(\Delta r)^2$, around the equilibrium position become important. To quantify this effect, we use the de Boer parameter $\Lambda = (\Delta r)^2/a^2$ [21], with $a = R/p \simeq 2R/\sqrt{n}$ being the mean interparticle separation, far from the boundary. As a rough estimate for $(\Delta r)^2$, we consider the harmonic approximation to the potential seen by a particle at the center ($r_p = 0$) of the structure, which can be expanded as

$$V(r) = 2\alpha/\pi \sum_{i=1}^{p-1} n_i K[(r/r_i)^2]/r_i$$
$$= \alpha/R\left(V_0 + \frac{1}{4}V_2\,(r/R)^2 + \cdots\right), \qquad (18)$$

with $V_k = \sum_{i=1}^{p-1} n_i/(r_i/R)^{k+1}$. The coefficients V_k are size-dependent and may be generally fitted by a series in $\sqrt{n}$. In particular, considering all equilibrium configurations with one particle at the center for $n \leqslant 400$, we obtain $V_2 \simeq A_2\, n^{3/2}\,[1 + O(1/\sqrt{n})]$ with $A_2 \approx 0.625$. In the harmonic approximation, one then has

$$m\omega^2 R^2 = \alpha V_2/(2R), \quad (\Delta r)^2 = \hbar/m\omega, \qquad (19)$$

providing the following estimate:

$$\Lambda^2 = \hbar^2/(m\alpha)\sqrt{\pi\sigma}/(8A_2) \qquad (20)$$

in terms of the particle density $\sigma = n/\pi R^2$. Quantum melting is avoided at $\Lambda \leqslant \Lambda_0 \sim 0.2$ [21], corresponding to an upper bound for the density, σ_0. As an example, we obtain for

electrons in GaAs ($m = 0.067m_e, \varepsilon_r \approx 12.4$) and $R = 1$ μm the onset of *cold melting* at $n \gtrsim 410$ particles, for which quantum corrections should be necessary.

In conclusion, we have derived a system of equations that enables one to analyze the equilibrium formation and filling of rings with a finite number of particles interacting by means of Coulomb forces in disk geometry. Our approach is based on the cyclic symmetry and periodicity of the Coulomb energy between particles located over different rings. As a result, the problem of n interacting charged particles is reduced to the description of p ($\ll n$) rings, with homogeneously distributed integer charges. This picture is good enough to obtain exact ground-state configurations with correct energies, excluding a few particular cases, up to $n \leqslant 105$. For bigger systems, the solution of the model equations provides also very good approximations to the exact ground-state configurations. Indeed, the energy errors do not exceed a small percentage fraction of the exact values. For $n \gtrsim 200$, our approach predicts the formation of the *hexagonal core* and *valence* circular rings for the centered configurations. The general evolution of the shell structure with an increasing number of particles is also properly described, including finite-size fluctuations. Note that the basic principles discussed for the disk geometry can also be applied to parabolic confinement, or any other circular potential. The computational effort to get global energy minima is much less than in MD or simulated annealing calculations. In fact, simulation times in these methods can be drastically reduced by feeding them with initial configurations obtained by means of our method. Finally, we have analyzed and quantified the range of applicability of a pure classical picture for the description of charged particles under hard circular confinement.

This work was supported in part by the Bogoliubov-Infeld program of BLTP and RFBR (Russian Federation), Grant 14-02-00723.

[1] J. J. Thomson, Philos. Mag. **7**, 237 (1904).
[2] M. J. Bowick and L. Giomi, Adv. Phys. **58**, 449 (2009).
[3] H. Saarikoski, S. M. Reimann, A. Harju, and M. Manninen, Rev. Mod. Phys. **82**, 2785 (2010).
[4] A. A. Koulakov and B. I. Shklovskii, Philos. Mag. B **77**, 1235 (1998); Phys. Rev. B **57**, 2352 (1998).
[5] A. Mughal and M. A. Moore, Phys. Rev. E **76**, 011606 (2007).
[6] Z. Yao and M. Olvera de la Cruz, Phys. Rev. Lett. **111**, 115503 (2013).
[7] B. P. Binks and T. S. Horozov, *Colloidal Particles at Liquid Interfaces* (Cambridge University Press, Cambridge, UK, 2006).
[8] M. E. Leunissen, A. van Blaaderen, A. D. Hollingsworth, M. T. Sullivan, and P. M. Chaikin, Proc. Natl. Acad. Sci. (USA) **104**, 2585 (2007).
[9] M. E. Leunissen, J. Zwanikken, R. van Roij, P. M. Chaikin, and A. van Blaaderen, Phys. Chem. Chem. Phys. **9**, 6405 (2007).
[10] E. P. Wigner, Phys. Rev. **46**, 1002 (1934).
[11] J. L. Birman, R. G. Nazmitdinov, and V. I. Yukalov, Phys. Rep. **526**, 1 (2013).
[12] E. Rousseau, D. Ponarin, L. Hristakos, O. Avenel, E. Varoquaux, and Y. Mukharsky, Phys. Rev. B **79**, 045406 (2009).
[13] V. M. Bedanov and F. M. Peeters, Phys. Rev. B **49**, 2667 (1994).
[14] Yu. E. Lozovik and V. A. Mandelshtam, Phys. Lett. A **165**, 469 (1992).
[15] F. Bolton and U. Rössler, Superlatt. Microstruct. **13**, 139 (1993).
[16] M. Kong, B. Partoens, A. Matulis, and F. M. Peeters, Phys. Rev. E **69**, 036412 (2004).
[17] A. A. Berezin, Nature (London) **315**, 104 (1985).
[18] A. Worley, arXiv:physics/0609231.
[19] M. Abramowitz and I. A. Stegun, *Handbook of Mathematical Functions with Formulas, Graphs, and Mathematical Tables*, 10th Printing, Applied Mathematics Series No. 55 (National Bureau of Standards, U.S. Government Printing Office, Washington, D.C., 1972), p. 590. $K(m) = \int_0^{\pi/2}[1 - m\sin^2\theta]^{-1/2}d\theta$.
[20] S. Erkoc and H. Oymak, Phys. Rev. E **62**, R3075(R) (2000); Phys. Lett. A **290**, 28 (2001).
[21] See, for example, D. I. Khomskii, *Basic Aspects of the Quantum Theory of Solids* (Cambridge University Press, New York, 2010), pp. 48–51.